Second-Harmonic Generation at the Upper Hybrid Layer in the ST Tokamak*

R. Cano,† C. Etievant,† and J. Hosea
Plasma Physics Laboratory, Princeton University, Princeton, New Jersey 08540
(Received 15 September 1972)

An extraordinary incident wave, propagating along the major radius through the ST tokamak plasma, is used to generate a second-harmonic wave inside the plasma. The detected harmonic-power characteristic agrees well with that predicted by the theory for local harmonic generation in the upper hybrid layer. The detected harmonic wave is essentially extraordinary, but has a small ellipticity.

A direct measurement of the current distribution in a tokamak plasma is particularly important for the determination of the magnetic shear and the location of singular magnetic surfaces in connection with the observed instabilities,[1,2] for the spatial resolution of the Joule heating, and for the evaluation of the component of current attributable to runaway electrons. In an earlier Letter,[3] it has been proposed that this measurement can in principle be effected by observing the polarization of the harmonic wave generated locally in the plasma with an electromagnetic wave polarized in the extraordinary mode and propagating perpendicularly to the toroidal magnetic field B_φ, along the major radius R (opposed to ∇B_φ). The existence of this mechanism of generation has been verified in the cold plasma of a high-frequency discharge.[4] In this earlier experiment, the electron temperature and density are well below those of the tokamak regime. In addition, the geometry is notably different from that of the tokamak. In this Letter, we describe the first experimental results of harmonic generation in the tokamak regime.

Figure 1 shows the experimental arrangement

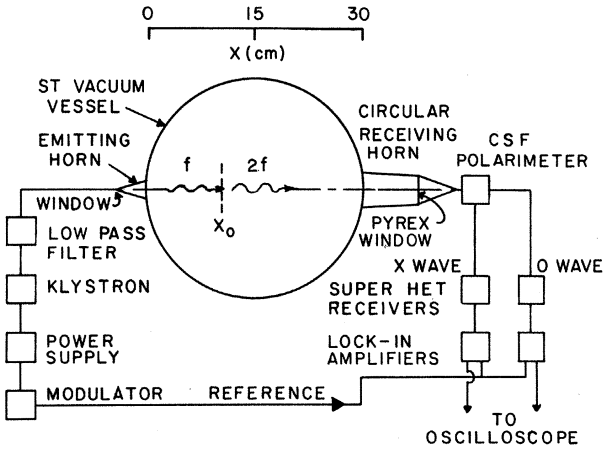

FIG. 1. Experimental arrangement for harmonic generation and detection on the ST tokamak.

used to launch the incident wave (f) and to detect the harmonic wave ($2f$) generated in the plasma of the ST tokamak.[5] The incident wave is provided by a klystron ($f = 34.6$ GHz) modulated at 20 kHz, which delivers up to 2–4 W of power. A low-pass filter eliminates the harmonic of the klystron, and only the fundamental wave (extraordinarily polarized) is launched by the emitting horn which is attached to the vacuum vessel.

The detection system for the harmonic wave employs a circular horn, located behind a Pyrex window and diametrically opposed to the incident horn, followed by a polarimeter (of the Finline coupler type) having a directivity between its two arms of 30–35 dB. Each arm is connected to a superheterodyne receiver followed by a lock-in amplifier which uses the klystron modulator signal as its reference. This system virtually eliminates detection of noise emitted by the plasma and can measure in a band of 1 kHz a minimum power of 5×10^{-12} W.

The polarimeter has been oriented in certain experiments at 45° in the "penumbra" fashion to give a good sensitivity for the rotations of the polarization. However, for most experiments, it has been aligned with B_φ thereby separating the ordinary and extraordinary components of the harmonic wave (Fig. 1).

Typical discharge conditions used in this study are given in Fig. 2(a). Small values of B_φ are dictated by the incident-wave frequency and, consequently, the modest current level is chosen to maintain a stable plasma.[2] The average electron density is set at $\sim 2.5\times10^{12}$ cm^{-3} to permit the measurement of harmonic polarization at the zone of harmonic generation.[3]

The detected signals are also shown in Fig. 2(a). An ordinary-to-extraordinary power ratio of $\sim \frac{1}{80}$ is evident in this case. The time dependence of the detected signals is not surprising since the density profile changes with time. (For the conditions of Fig. 2, the extraordinary chan-

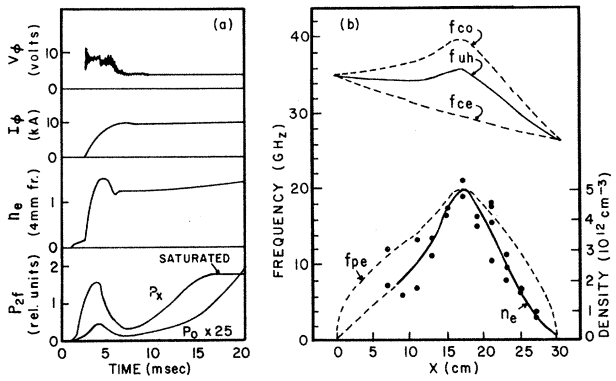

FIG. 2. Characteristics for a helium discharge with $B_\varphi = 10.82$ kG and a current channel radius of 12 cm. (a) V_φ, I_φ, interferometer density, and the extraordinary (P_x) and ordinary (P_0) components of the detected harmonic power P_{2f} versus time. (b) Thomson scattering measurements of electron density and calculations of the characteristic frequencies versus x (Fig. 1) for $t = 11$ msec.

nel is saturated late in time.)

Figure 2(b) gives Thomson scattering measurements of electron density for $t = 11$ msec. (The temperature profile is similarly peaked and has a maximum value of $T_e \sim 200$ eV.) The zero-order density curve (solid) is obtained by folding the data about $x = 17$ cm (neglecting the innermost points which are in doubt because of enhanced stray laser light). Linear projections are used to complete the curve outside the range of the laser. The corresponding profiles of the plasma (f_p), cyclotron (f_{ce}), upper hybrid (f_{uh}), and cutoff (f_{co}) frequencies are illustrated.

With the incident-wave frequency maintained constant, we have varied the zone of interaction by changing the level of B_φ. Transmission measurements reveal that the plasma is totally opaque to the incident wave when the incident frequency falls between the minimum cyclotron frequency ($x = 30$ cm) and the maximum cutoff frequency [Fig. 2(a)], and that transmission rapidly ensues when the incident wave no longer encounters this nonpropagating region.

In Fig. 3, we show the detected power at 11 msec (conditions of Fig. 2) for the extraordinary component of the harmonic wave as a function of $B_{\varphi 0}$, or equivalently f_{ce0}, the cyclotron frequency at the center of the vessel ($x = 15$ cm, $R = 109$ cm). For comparison, we present the cross section for harmonic generation at the upper hybrid layer[6] for the density curve of Fig. 2(b),

$$M^2 = \left| \frac{f_{ce}}{f} \frac{f_p^2}{\partial f_{uh}^2/\partial x} \left[\frac{f_{ce}^2}{f_{co}^2 - f_{uh}^2} \right] \right|_{x = x_0} \text{cm}^2, \qquad (1)$$

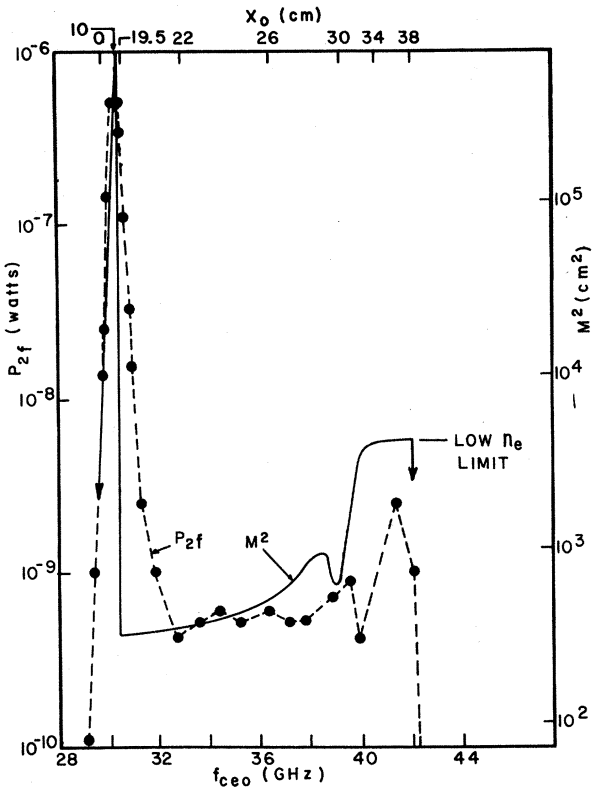

FIG. 3. Detected harmonic power P_{2f} for $t = 11$ msec versus the cyclotron frequency (magnetic field) at the center of the vessel f_{ce0}. (Discharge conditions are those of Fig. 2.) M^2 of Eq. (1), calculated for the density profile of Fig. 2, is also shown.

where x_0 is the position of the resonance layer (Fig. 1). M^2 relates the incident and harmonic Poynting vectors at the resonance layer,

$$S_{2f}|_{x=x_0} = (128\pi e^2/m_e^2 c^5) M^2 S_f^2|_{x=x_0} \text{ erg sec}^{-1}\text{ cm}^{-2}. \qquad (2)$$

We find that the qualitative dependences of the measured P_{2f} and the calculated M^2 are identical in three respects. First, we note that $M^2 \to \infty$ when $\partial f_{uh}^2/\partial x \to 0$ and, in fact, an enhancement of 3 orders of magnitude is observed for P_{2f} in the vicinity of the value of f_{ce0} which gives $\partial f_{uh}^2/\partial x = 0$, where $f = f_{uh}$ [see Fig. 2(b)]. Secondly, for larger values of $f_{ce0}(B_{\varphi 0})$, the emission exhibits a plateau which agrees well with the slowly increasing value of M^2. Finally, for $f_{ce0} > 39.6$ GHz, corresponding to resonance in the port extension leading to the Pyrex window in front of the receiving horn (Fig. 1), an enhancement in emission is observed and an enhancement of M^2 is predicted. $M^2 \to (R/2)^2$, independent of electron

density, in this low-density region where $f_p^2/f_{ce}^2 \ll 1$.

The transition of M^2 from its peak to plateau is faster than that for P_{2f}. Possible contributors to this difference are that the actual density profile differs in local detail from the zero-order curve used and that the theory is approximate.[6] Also, M^2 does not approach zero as $n_e \to 0$, as noted above. A more exact theoretical treatment, valid for low densities and including dissipation effects, should give the proper behavior.

In the region of the plateau of Fig. 3, the absolute value of $P_{2f} \simeq 5\times10^{-10}$ W compares very favorably with that calculated for $M^2 \simeq 300$. The power at the receiving horn is[6]

$$P_{2f} \simeq 4.6\times10^{-15} M^2 P_f^2 G_1^2 A_2/(4\pi x^2)^2 \quad \text{erg sec}^{-1}, \qquad (3)$$

where G_1 is the gain of the emitting horn and A_2 is the aperture of the receiving horn. Upon taking into account the measured losses of the emission and reception circuits, we calculate $P_{2f} \simeq 6\times10^{-10}$ W. This almost-perfect agreement would appear to be fortuitous since Eq. (3) omits diffraction and/or refraction by the plasma, and since Eq. (2) is not exact. However, we are indeed measuring harmonic powers indicative of harmonic generation at the upper hybrid layer.

The value of f_{ce0} for which M^2 is a maximum depends on the slope of the density profile in the region of small x [Fig. 2(b)]. If a given symmetric profile (about $x = 15$ cm) maintains its shape as the maximum density is decreased, the maximum of M^2 is displaced to larger values of $f_{ce0} \times (B_{\varphi 0})$. This property has been observed experimentally, as shown in Fig. 4, for a plasma maintained approximately at the center of the vessel by monitoring poloidal-field position loops.[2,7] The theoretical curve which best fits the data (Fig. 4) is for a density profile of the form $n = n_0 \sin(\pi x/30)$, where n_0 is determined from microwave interferometer measurements.

The measurements of the polarization of the harmonic give $(P_{2f})_0/(P_{2f})_x \sim 10^{-2}$ over a wide range of operating conditions, confirming that the harmonic is essentially extraordinary. The existence of a small ordinary component which cannot be nulled shows that the wave leaving the vessel possesses a slight ellipticity. This ellipticity is largely independent of the discharge conditions and presumably is due to reflections inside the vessel and the receiver horn.

The ensemble of measurements presented above strongly supports the theory of local harmonic generation in the upper hybrid layer. Consequently, the principle that *local* measurements are permitted across the plasma by varying B_φ or the incident frequency is established.

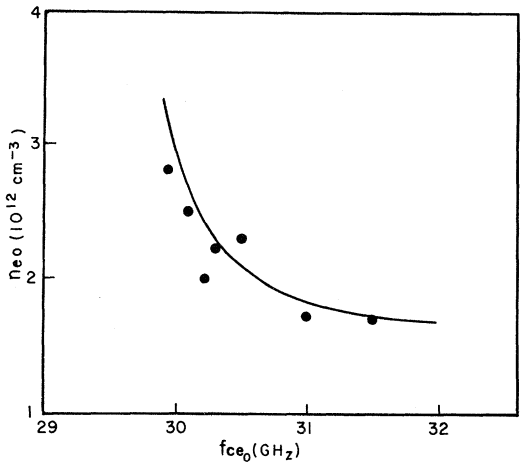

FIG. 4. The peak electron density versus f_{ce0} corresponding to the maximum harmonic emission from a hydrogen discharge, compared to M^2 for a sinusoidal density profile.

The rotation of the plane of polarization of the generated harmonic due to the poloidal field produced by the toroidal current in the plasma is an order of magnitude smaller than the presently observed ellipticity. An adequate measurement of the current distribution can be made with a polarimeter oriented at 45° relative to B_φ if this ellipticity can be reduced by an order of magnitude. We think that this reduction can be achieved by taking special precautions to eliminate spurious signals resulting, for example, from reflections from the vessel wall and windows.

We wish to thank Professor M. Gottlieb and Dr. M. Trocheris for their encouragement and support, Dr. I. Fidone for suggesting the experiment, and Professor H. Furth and Dr. E. Meservey for their interest. We also thank M. A. Bresson for his assistance with the preparations for the experiments, Dr. L. Johnson for providing the laser profiles. Dr. R. Motley and Dr. M. Schwartz for valuable discussions, and the support staff of the ST tokamak for their invaluable assistance.

*Work supported by the U. S. Atomic Energy Commission under Contract No. AT(11-1)-3073 and by the

Association Centre à l'Energie Atomique–EURATOM, Fontenay-aux-Roses, France. Use was made of computer facilities supported in part by National Science Foundation Grant No. NSF-GP579.

†Permanent address: Centre d'Etudes Nucléaires, Fontenay-aux-Roses, France.

[1]S. V. Mirnov and I. B. Semenov, At. Energ. 30, 20 (1971) [Sov. At. Energy 30, 22 (1971)].

[2]J. C. Hosea, C. Bobeldijk, and D. J. Grove, in *Proceedings of the Fourth International Conference on Plasma Physics and Controlled Nuclear Fusion Research* (International Atomic Energy Agency, Vienna, 1972), Vol II, p. 425.

[3]R. Cano, I. Fidone, and M. J. Schwartz, Phys. Rev. Lett. 27, 783 (1971).

[4]R. Cano, G. Chaignot, I. Fidone, and M. J. Schwartz, EURATOM–Centre à l'Energie Atomique Report No. EUR-CEA FC-620 (to be published).

[5]Reference 2 and pertinent references therein give a more thorough description of the ST device.

[6]I. Fidone, G. Granata, and J. Teichmann, Phys. Fluids 14, 737 (1971).

[7]S. V. Mirnov, At. Energ. 17, 209 (1964) [J. Nucl. Energy, Part C 7, 325 (1965)].

Particle Motion in Magnetic Mirrors with High-Frequency Electric Field Fluctuations

R. E. Aamodt*
Department of Astro-Geophysics, University of Colorado, Boulder, Colorado 80302

and

J. A. Byers†
Lawrence Livermore Laboratory, University of California, Livermore, California 94550

(Received 7 August 1972)

Particle motion in a magnetic mirror containing high-frequency short-wavelength longitudinal electric fields is followed numerically for many mirror bounce periods. It is found that while the magnetic moment undergoes large rapid changes, these fluctuations seldom imply rapid particle loss from the mirror. This behavior is shown to be completely consistent with nonlinear superadiabatic theory, wherein containment properties of the trap are affected only when particles cross isolated singular surfaces in phase space.

Microinstabilities for warm plasma contained by magnetic mirrors are typically characterized by longitudinal electric fields having frequencies near multiples of the ion cyclotron frequency, and wavelengths, in units of the ion gyroradius, long along and short across the external $\vec{B}$ field. The all-important question of particle containment in such fields is a difficult one and must be attacked by both numerical and analytic methods. In this Letter we report the results of a study where, for a small set of initial conditions, we numerically follow particle motions for many mirror cycles under various field conditions. These results are shown to be consistent with an approximate averaged analytic theory. Also, the details of the numerical results have enabled us to determine the relative importance of various aspects of the theory.

The basis of the approximate analytic theory is that, while the magnetic moment is no longer an adiabatic invariant in such fluctuations, an invariant still exists almost everywhere along the particle's trajectory.[1] According to this "superadiabatic" theory, it is only when a particle is forced to cross an isolated singular surface (separatrix) in phase space that this invariant is broken and a nonperiodic change induced in the particle's mirror motion. Containment of a particle, once contained in this field configuration, is then determined by the accumulative sum of these nonadiabatic transitions along the entire path history of the particle.

The field configuration used in the simulation has been chosen to be a divergence- and curl-free weak magnetic mirror field with components $B_Z(X, Z)$ and $B_X(X, Z)$, where $B_Z \gg B_X$, and an electric potential $\varphi(Z, X, t)$ with frequency chosen to be near the minimum of the second harmonic of the cyclotron frequency. In these functionally fixed fields, the exact equations of motion are numerically solved using a standard simulation numerical algorithm with a corrector that renders the orbit exact if all fields were independent of X, Z, t.[2] With these techniques, particle trajectories with differing initial phases have been calculated for times up to $10^5/2\pi$ cy-